E7-FW, GATGGTCCAGCTGGACAAGC; HPV16 E7-RV, GTGCCCATTAACAGGTCTTC; actinF, TCAGAAGGATTCCTATGTGG; actinR, TCTCCTTAATGTCACGCACG.

Western blot analysis was performed with 20 μg protein from whole-cell extracts separated by sodium dodecylsulfate–polyacrylamide gel electrophoresis, and blotted on Immobilon P filters (Millipore, Bedford, MA, USA). The following antibodies were used: anti p16 (clone G175-405, BD Biosciences, San Jose, CA, USA), anti p53 (clone DO-1, Oncogene Science, Cambridge, MA, USA) and antimouse IgG, HRP-linked antibody (Cell Signaling, Danvers, MA, USA). Lumi-Light Plus Western Blotting Substrate (Roche, Manheim, Germany) was used for detection.

### Telomeric repeat amplification protocol assay and telomere length analysis by Southern blotting

Telomeric repeat amplification protocol (TRAP) assays were performed using the Trapeze telomerase detection kit (Intergen, Purchase, NY, USA) according to the manufacturer's protocol. DNA was extracted from B cells using the Qiamp DNA Blood Mini kit (Qiagen) according to the manufacturer's instructions, and the telomere length was analyzed using Southern blot analysis with a TeloTAGGG Telomere Length Assay (Roche), according to the manufacturer's protocol.

### Cell cycle analysis by flow cytometry

A total of $5 \times 10^5$ cells were washed with PBS, fixed on ice with 70% ethanol for 30 min, washed again with PBS, and incubated with 100 μg/mL RNAse A solution (Qiagen). The cells were centrifuged, washed again with PBS, and then incubated with propidium iodide (5 μg/mL: Pharmingen) on ice for 20 min. Finally, the DNA contents were analyzed by flow cytometry as previously described.

### Karyotype analysis

A karyotype analysis was performed at late passage (19 months) for each cell line. Routine karyotypic analysis was performed using preparations stained with 5% Giemsa solution. In order to identify possible rearrangements, chromosomes of metaphases were G-banded. For each cell line, more than 50 cells were scored for their chromosome number.

### Immunophenotyping and *in situ* hybridization for EBV

Immunophenotyping and *in situ* hybridization were also performed at late passage (19 months) for each cell line. Cells were fixed in 10% formaldehyde and embedded in paraffin. The avidin–biotin–peroxidase complex method was used for all immunohistochemical studies. Primary antibodies and the probe used were as follows: polyclonal CD3, L26 (CD20), mb-1 (CD79a), IgM, IgG, IgA, κ, λ, Bcl2 and Bcl6 (Dako, Copenhagen, Denmark), CD5, CD10, cyclin D1 and EBV probe for EBV-encoded RNA (Novocastra, Newcastle, UK). *In situ* hybridization was performed according to the manufacturer's protocol with slight modifications.

## RESULTS

### Culture, growth curve and expression of HPV16 E6 and E7

Co-cultured with CD40L-expressing and irradiated NIH3T3, primary human B lymphocytes entered into the cell cycle and then began to grow, forming cell clusters (Fig. 1a). Next, these cells were infected with retrovirus vectors expressing HPV16 E6E7 or control EGFP, and the culture was continued with CD40L-NIH3T3 cells. The efficient infection of retrovirus vectors into activated human B lymphocytes was demonstrated by EGFP signals (Fig. 1b). Without transduced genes, human B lymphocytes ceased to grow around 10 population doublings (PDL; around day 25–30; Fig. 1c) with the accumulation of p16 protein, an inhibitor of Cdk4/6 (Fig. 1d). In clear contrast, E6E7-transduced B cells were able to proliferate for more than 2 years (>100 PDL; Fig. 2). By RT-PCR, the expression of E6E7 mRNA was detected in the E6E7 vector-transduced cells in both early and late passages (Fig. 3). Surprisingly, EGFP-transduced cells were also able to proliferate for more than 2 years although at a slower proliferation rate (Fig. 2). We first considered that EBV infection might be attributable to the continuous proliferation of the EGFP-transduced B lymphocytes. However, *in situ* hybridization for EBV-encoded RNA was negative, and we could not detect any EBV-DNA even by real-time quantitative PCR (data not shown).

### Telomerase activity and telomere length

We investigated telomerase activity in these cells using a TRAP assay. Both E6E7-transduced cells and EGFP-transduced cells had a high telomerase activity both in the early and late passage (Fig. 4a). We then measured the telomere length by Southern blotting. The average telomere lengths of E6E7-transduced cells or EGFP-transduced cells were 8–10 kb, irrespectively of passage periods (Fig. 4b). Together, both E6E7-transduced cells and EGFP-transduced cells were considered to be immortalized.

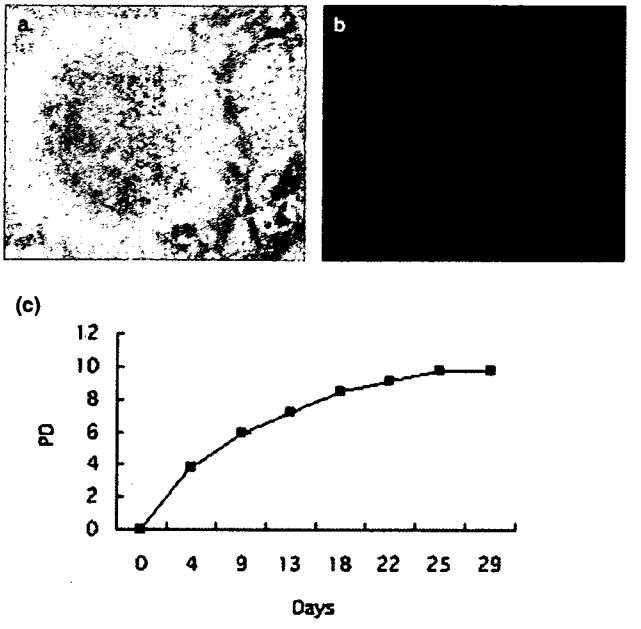


**Figure 1** p16-related growth arrest in long-term culture of human primary B lymphocytes. The morphological features of human primary B lymphocytes cultured on CD40L expressing NIH 3T3 cells. Cluster formation is seen. (**a**) Morphological features of enhanced green fluorescent protein (EGFP)-transduced B lymphocytes. (**b**) Growth curve of human primary B lymphocytes. The cells stopped proliferating at 9–10 population doublings (PD). (**c**) Western blot analysis of p16 protein. p16 accumulation is observed from day 9, and continues to increase until growth arrest at day 25–29. Cell lysate of human foreskin keratinocyte (HFK) was included for positive control.

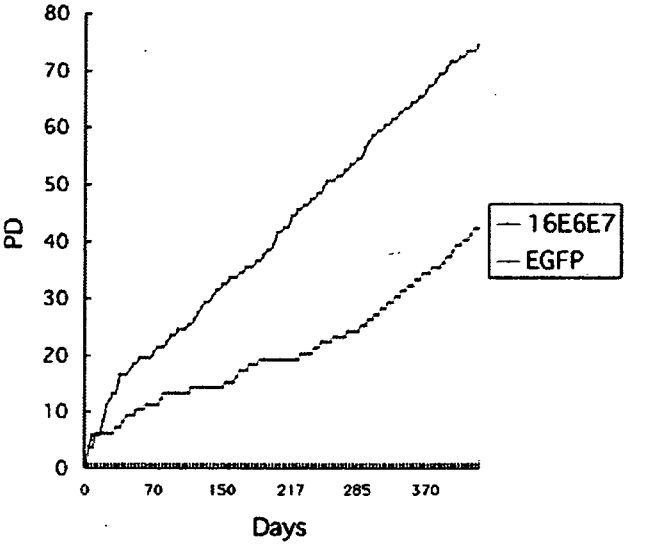


**Figure 2** Growth curve of 16E6E7- or enhanced green fluorescent protein (EGFP)-transduced B cells. PD, population doubling.

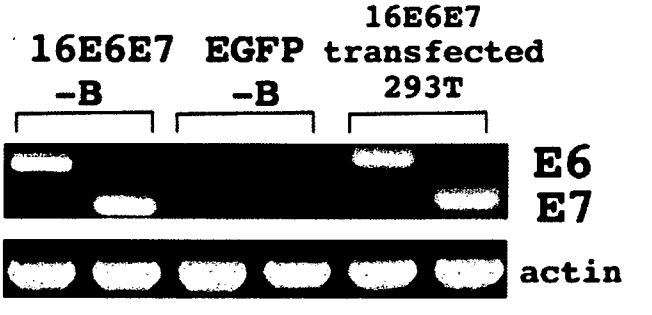


**Figure 3** Reverse transcription–polymerase chain reaction (RT-PCR) analysis of 16E6E7- or enhanced green fluorescent protein (EGFP)-transduced human B cells. PCR product of 243 bp and 143 bp for E6 and E7, respectively, are detected in 16E6E7-transduced cells.

### Expression of p16 protein

As described in the previous section, it is conceivable that the accumulation of p16 protein may cause cell cycle arrest in cultured primary B-cells (Fig. 1c,d). Therefore, we examined the p16 protein levels in E6E7- or EGFP-transduced immortalized B cells (Fig. 5). A comparable accumulation of p16 to that in presenescent B cells was observed in the E6E7-transduced immortalized B cells. This finding suggests that E7 directly binds and inactivates Rb and thereby cancels the inhibitory effect of p16 in B cells, and this finding is consistent with previous findings observed with other cell types. Interestingly, the p16 level decreased in the EGFP-transduced immortalized cells. We considered that cells in which p16 expression has been spontaneously downregulated are selectively immortalized. Such a phenomenon is observed also in HMEC, where the p16 mRNA expression is suppressed by the methylation of the promoter region.[32] We therefore performed a PCR-based analysis to investigate the methylation status of the p16 promotor region in the EGFP-transduced immortalized cells, but no methylation was found (data not shown). We also examined the p53 protein levels in these cells (Fig. 5). In the E6E7-transduced cells, the p53 protein levels decreased, which was an indication that p53 is also degraded by E6 in B lymphocytes. In EGFP-transduced B cells, p53 protein levels were unchanged, thus suggesting that the status of p53 protein was not associated with the spontaneous immortalization of EGFP-transduced cells.

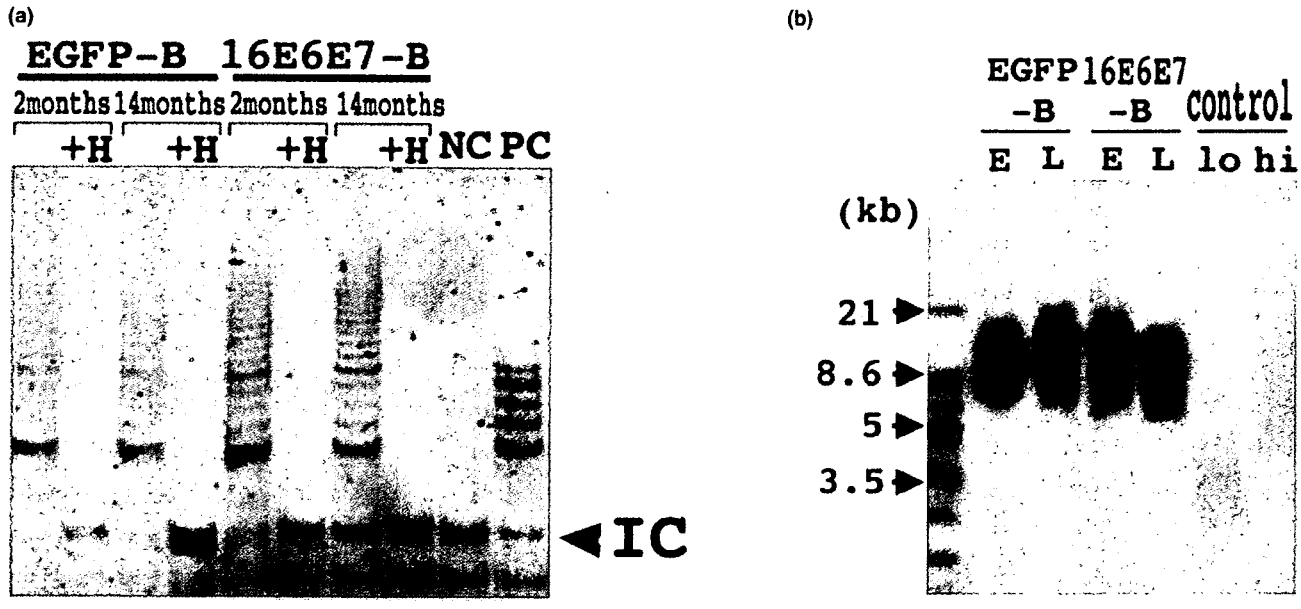


**Figure 4** Analysis of the telomerase activity and telomere length of 16E6E7- or enhanced green fluorescent protein (EGFP)-transduced B cells. (**a**) Telomeric repeat amplification protocol (TRAP) assay of early (2 months) or late (14 months) passage of 16E6E7- or EGFP-transduced human B cells. A high telomerase activity is seen in early/late passage and in EGFP/16E6E7-transduced cells. +H, heat-inactivated negative control for each sample; IC, internal control (to normalize the efficiency of PCR amplification); NC, negative control; PC, positive control. (**b**) Southern blot analysis of early (2 months) or late (14 months)-passage 16E6E7- or EGFP-transduced B cells. Terminal restriction fragments are visualized using a probe against the telomeric repeat sequence. The size standard is indicated at the left. E, early passage; hi, control DNA with high-molecular-weight telomeres; lo, control DNA with low-molecular-weight telomeres; L, late passage.

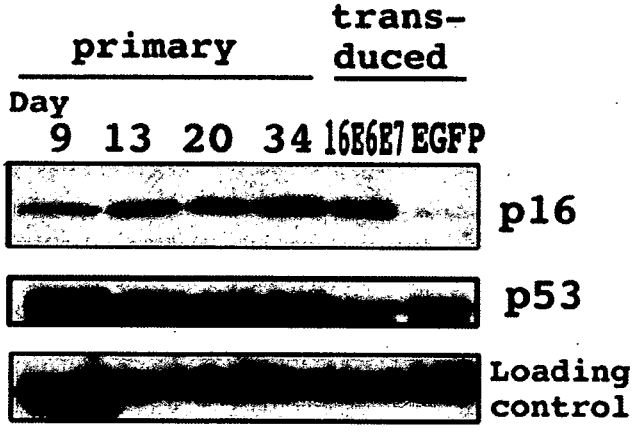


**Figure 5** Western bot analysis of p16 and p53 in primary or 16E6E7/enhanced green fluorescent protein (EGFP)-transduced B cells. A total of 20 μg protein from whole-cell extracts on day 9, 13, 20, 34 of the cultured primary B cells is loaded on the left side for control. And 20 μg protein from whole-cell extracts of late passage (14 months) 16E6E7- or EGFP-transduced B cells are loaded on the right side.

### RNA interference analysis

Three transcription variants are known to encode the E6 and E7 proteins in the HPV genome. E7 protein is generated from all three variants but, because two introns exist within the E6 coding sequence, full-length E6 protein is generated only from one variant that encodes both full-length E6 and E7.[28] We thus constructed shRNA expressing retroviral vectors that could silence the expression of either E6 alone or both E6 and E7 (Fig. 6a). CaSki cells expressing HPV16 E6 and E7 were first subjected to knockdown of E6 alone by expressing E6-specific shRNA (E6Ri3) or both E6 and E7 by expressing another shRNA (E7Ri2). Protein levels of E7 protein or p53 protein were analyzed by western blotting because the expression of p53 protein is normally reduced by E6 protein. Compared with Hela cells that do not contain the HPV16 genome, the upregulation of p53 was observed by the introduction of E6-specific shRNA or E7-shRNA but not by control vector, and reduction of E7 protein was observed by the introduction of E7-shRNA but not by E6-specific shRNA or control vector. We next infected E6E7-transduced B cells with the same set of retroviruses. After infection and drug selection by puromycin, control cells and E6 knocked-down cells were able to proliferate again, but the E6/E7 knocked-down cells all died within 1 week (Fig. 6). We infected EGFP-transduced B cells with the same set of viruses, but all cells remained healthy and proliferative after drug selection, thus indicating that the cell death in E6E7-transduced B cells was not caused by non-specific cell damage during retroviral infection and drug selection. To further investigate the mechanism of cell

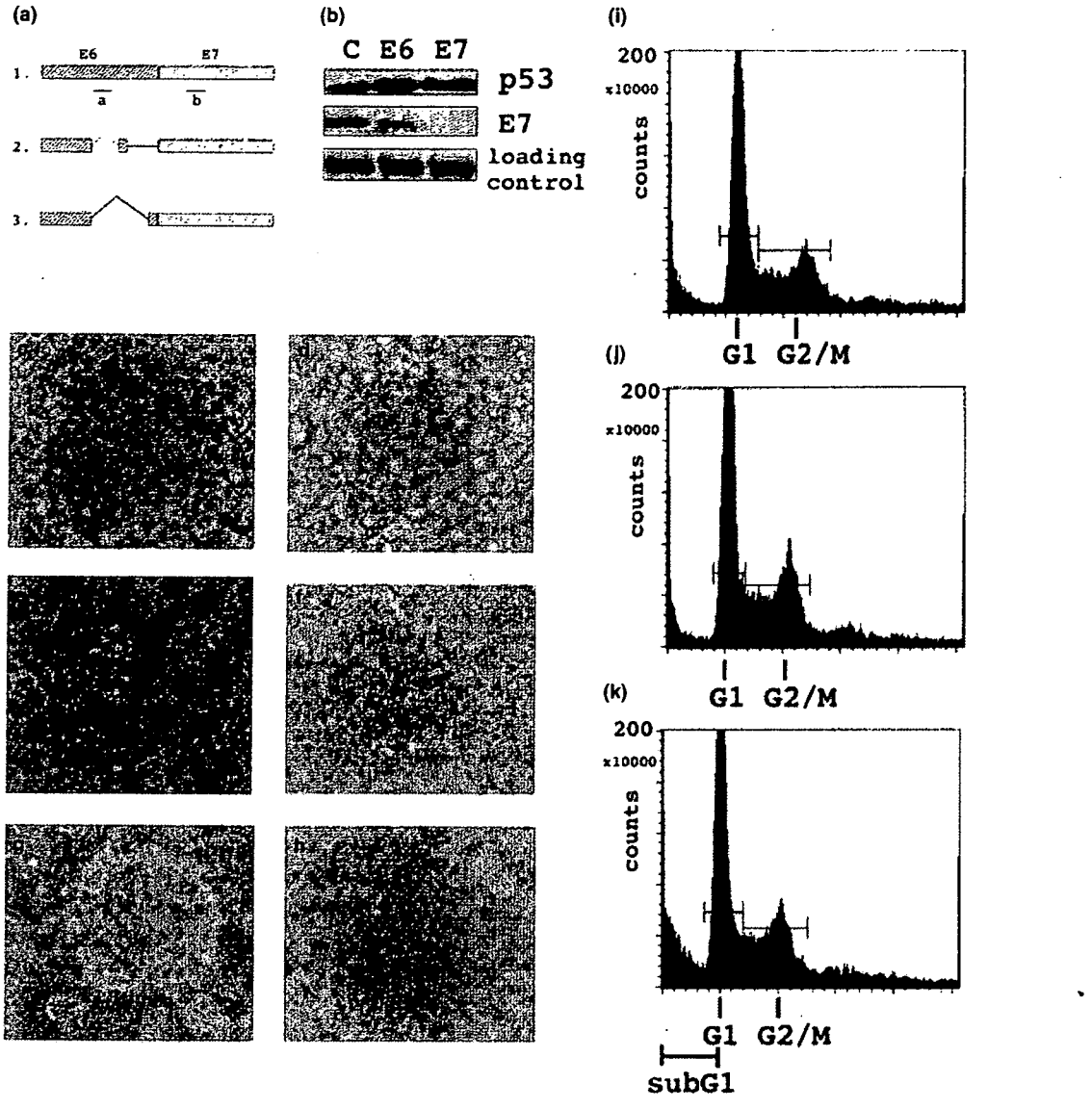


**Figure 6** RNA interference analysis of E6 alone or both E6 and E7 knockdown in 16E6E7- or enhanced green fluorescent protein (EGFP)-transduced B cells. (**a**) Three transcription variants (1–3) of HPV16E6E7 and the location of the target sequences for short hairpin RNA (shRNA; a: E6Ri3, b: E7Ri2). Knockdown of only variant 1 occurs by E6Ri3, and knockdown of all variants occur by E7Ri2. (**b**) Efficiency of shRNA constructs. ShRNA (E6Ri3 and E7Ri2) were transduced into SiHA cells by retroviral transduction. The upregulation of p53 by E6 silencing occurs in transduction of either E6Ri3 or E7Ri2, but knockdown of E7 occurs only in E7Ri2. C, control vector; E6, E6Ri3; E7, E7Ri2. (**c–h**) Retroviral transduction of shRNAs. Late-passage (12 months) 16E6E7- or EGFP-transduced B cells were further retrovirally transduced with shRNA constructs or retroviral vector. Drug selection using puromycin was done for 5 days after second infection. (**c**) 16E6E7-transduced B cells/negative control; (**d**) 16E6E7-transduced B cells/E6Ri3; (**e**) E7Ri2; (**f**) EGFP-transduced B cells/negative control; (**g**), EGFP-transduced B cells/E6Ri3; (**h**) EGFP-transduced B cells/E7Ri2. (**i–k**) Cell cycle analysis of shRNA transduced 16E6E7-transduced B cells. Late-passage (12 months) 16E6E7-transduced B cells were retrovirally transduced with shRNA constructs or retroviral vector: (**i**) control vector; (**j**) E6Ri3; (**k**) E7Ri2. No drug selection was performed, and flow cytometric analysis of DNA content stained by propidium iodide was performed 2 days after infection. A total of 30 000 cells were counted.

death by E6/E7 knockdown, a cell cycle analysis was performed. SubG1 fraction of E6/E7 knocked-down cells were more than twofold larger (17%) than the control cells (7.3%) and E6-only knocked-down cells (5.1%; Fig. 6), thus indicating that E6/E7 knockdown resulted in the apoptosis of E6E7-transduced B cells.

### Karyotype analysis

Although a karyotype analysis was performed in late passage cell lines, 50% of HPV16E6E7-transduced cells (25/50 cells) had the normal set of 46 chromosomes (Fig. 7). The chromosomal number of 20% of the cells (10/50 cells) was 47 and

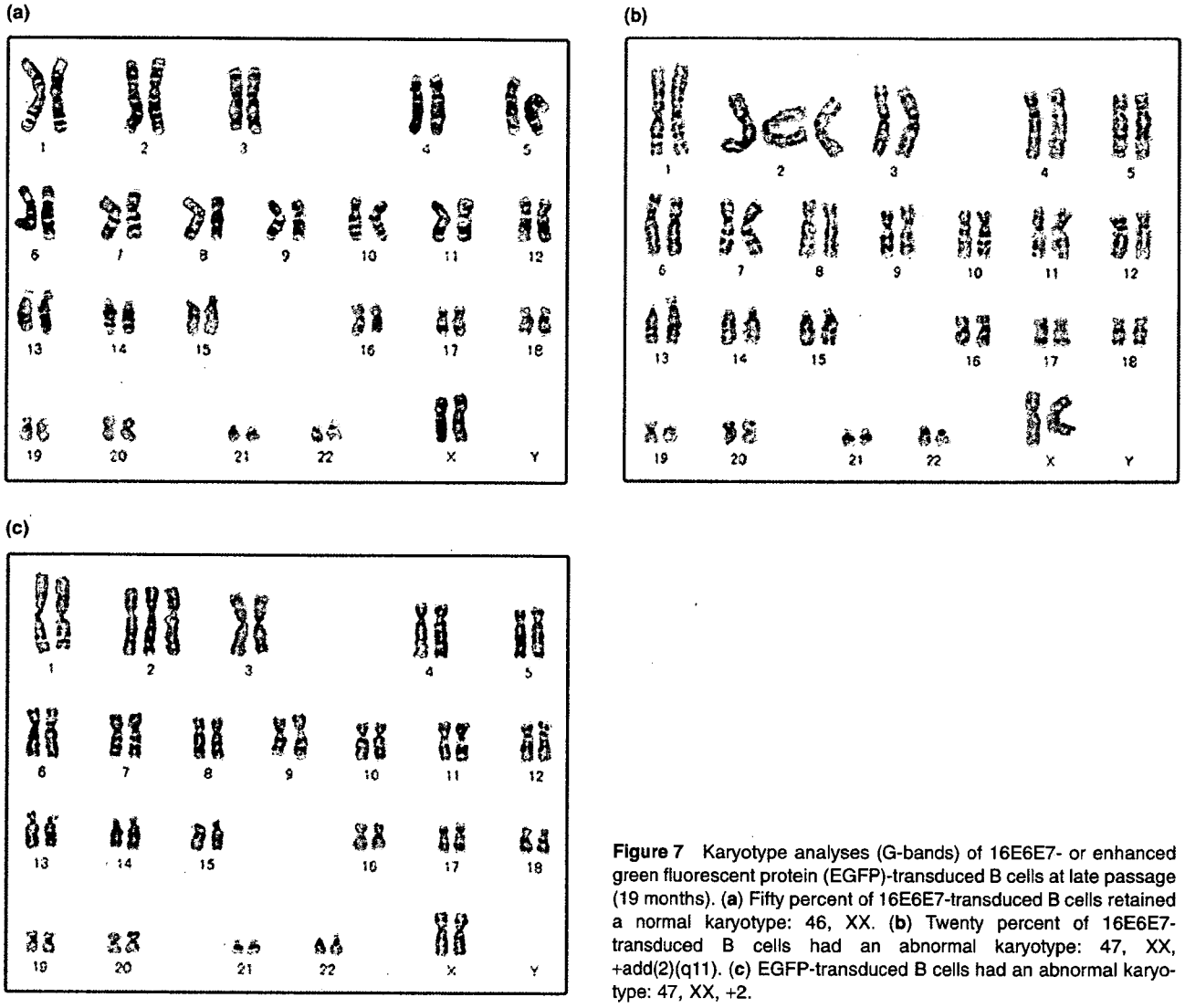


**Figure 7** Karyotype analyses (G-bands) of 16E6E7- or enhanced green fluorescent protein (EGFP)-transduced B cells at late passage (19 months). (**a**) Fifty percent of 16E6E7-transduced B cells retained a normal karyotype: 46, XX. (**b**) Twenty percent of 16E6E7-transduced B cells had an abnormal karyotype: 47, XX, +add(2)(q11). (**c**) EGFP-transduced B cells had an abnormal karyotype: 47, XX, +2.

that of residual cells varied from 90 to 95. G-banding revealed that cells with 46 chromosomes had a normal karyotype: 46 XX (10/10 cells); and cells with 47 chromosomes had a common abnormality: 47 XX add (2)(q11) (6/6 cells). All analyzed cells of EGFP-transduced cells (50/50 cells) had 47 chromosomes with a common karyotypic abnormality: 47 XX, +2 (10/10 cells).

### Immunophenotyping and *in situ* hybridization

Both E6E7-transduced cells and EGFP-transduced cells were positive for B-cell markers such as CD20 and CD79a, and negative for CD3, confirming that the immortalized cells retained the B-cell phenotype. Both cell lines were also positive for bcl-2, bcl-6, and CD10, and negative for either CD5 and cyclin D1, phenotypically similar to follicle center cells. Furthermore, E6E7-transduced cells were mostly positive for IgA and λ, and EGFP-transduced cells were mostly positive for IgG and λ. Both cells were negative for EBV-encoded RNA (data not shown).

## DISCUSSION

In the present study we successfully established EBV-negative cell lines derived from human primary B lymphocytes immortalized by HPV16 E6 and E7. This was unexpected, because human B cells were predicted to be difficult to immortalize, given the previous evidence that they require at least five EBV proteins for immortalization/transformation.[17–20] We also demonstrated for the first time that p16 protein is upregulated during the long-term culture of primary human B lymphocytes in a CD40-CD40L system.

This was understandable because the accumulation of p16 is a common feature observed in senescent fibroblasts, HMEC, keratinocytes, and T lymphocytes.[10,33,34] Although Herbert *et al.* proposed that p16 accumulation merely reflects an inappropriate culture condition (culture stress-induced growth arrest),[35] more recent experiments by Rheinwald *et al.* confirmed that p16-related arrest mechanism does exist in their system, with a p53-dependent component.[36] We therefore consider that whatever the cause of the p16-related arrest mechanism, the long-term culture of primary human B lymphocytes is also regulated by a telomere-independent, p16-related arrest mechanism that precedes the senescence induced by the shortening of telomere length.

Unexpectedly, EGFP transduced B cells also had a prolonged lifespan. We consider that this was because, similar to HMEC, p16 downregulated clones were selected and the activation of telomerase occurred by CD40–CD40L interaction. The telomerase activity is induced *in vitro* in B lymphocytes by stimulation via antigen receptor[37] or CD40–CD40L interaction, which mimics antigen–antigen receptor interaction.[38] In the present study we demonstrated that both cell lines showed a high telomerase activity in either the early or late passage, and we consider that an upregulation of the telomerase activity occurs in B lymphocytes cultured in this CD40–CD40L system, which is consistent with previous reports. It is therefore unlikely that clones were selected because of an upregulated telomerase activity. The reason for the downregulation of p16 protein is unclear. Because no methylation of the p16 promotor CpG island was detected, we speculate that an upregulation of the proteins that downregulate p16 may thus have occurred spontaneously. Further studies, however, are necessary to elucidate this point.

E7, and probably not E6, was therefore necessary for immortalization by HPV16 E6 and E7. This is explained by the aforementioned reasons. The upregulation of the telomerase activity occurs in B lymphocytes cultured in this CD40-CD40L system. E6 induces the telomerase activity in epithelial cells[39] and human T lymphocytes (Y Yamashita, T Kiyono, unpubl. obs. 2001), and degrades p53 in epithelial cells[40] and lymphocytes (Fig. 6). However, in the present system and in a previously reported system,[38] the telomerase activity was efficiently induced by CD40–CD40L stimulation. Interestingly, a recent report demonstrated that CD40–CD40L interaction is a critical effector in EBV-related cell survival and transformation.[41] We therefore consider telomerase induction by CD40–CD40L interaction to be a very important factor in B lymphocyte immortalization and, similar to epithelial cells, such as HMEC, it is an additional step that contributes to inactivation of the Rb pathway that is required for immortalization.

Although we started the culture in a bulk culture system with polyclonal B lymphocytes confirmed by a conventional nested PCR method using FrIII and LJH/VLJH primer,[42] clonal bands were observed by the same method, thus showing that established cell lines contained clonal populations (data not shown). This is explainable in the case of EGFP-transduced cells because in these cells, a clone with downregulated p16 was selected. The reason for the clonality in E6E7-transduced cells is unclear, but karyotypic analyses showed that HPV16 E6E7-transduced cells were polyclonal in contrast to clonal EGFP-transduced cells. Furthermore, according to a most recent report, human hematopoietic cells were immortalized by HPV16 E6E7 either alone or in concert with hTERT, and were either oligoclonal or clonal judged by a chromosomal analysis.[43] We speculate that in such long-term cultures, dominant clones are selected by subtle growth advantages.

Our findings should be a start for investigating precise steps required for B-cell immortalization, especially by EBV. *LMP1* perturbs the p16/Rb pathway in human fibroblasts and B cells by promoting the nuclear export of Ets2 and E2F4/5.[44] Recently, the expression of CD40L by EBV was found in LCL,[41] thus the CD40–CD40L interaction should occur stably in LCL. These findings together with our results suggest that LCL should easily be immortalized by EBV. However, this seems not to be true according to previous lines of evidence.[16] The reason for this discrepancy remains to be clarified. It will be interesting to determine whether LMP1 alone can immortalize B cells in the CD40–CD40L system.

In conclusion, we have showed that human primary B lymphocytes were successfully immortalized by HPV16 E6 and E7, with E7 playing the most important role by destroying the Rb pathway. CD40–CD40L interaction also participates in B-cell immortalization by activating telomerase. We thus conclude that the steps required for B-cell immortalization at least in culture are closely similar to HMEC in which two steps (the inactivation of the Rb pathway and the maintenance of the telomere length), are required for immortalization.

## ACKNOWLEDGMENTS

The authors thank Kyoko Kato-Bunno, Chiemi Fujinaka and Nobuaki Misawa for expert technical assistance, and the former members of the Division of Virology, Aichi Cancer Center Research Institute, for helpful advice.

## REFERENCES

1 Hayflick L. The limited *in vitro* lifespan of human diploid cell strains. *Exp Cell Res* 1965; **37**: 614–21.
2 Ishikawa F. Cellular senescence, an unpopular yet trustworthy tumor suppressor mechanism. *Cancer Sci* 2003; **94**: 944–7.
3 Itahana K, Campisi J, Dimri GP. Mechanisms of cellular senescence in human and mouse cells. *Biogerontology* 2004; **5**: 1–10.
4 Sherr CJ. Principles of tumor suppression. *Cell* 2004; **116**: 235–46.

5 Miller G. Immortalization of human lymphocytes by Epstein-Barr virus. *Yale J Biol Med* 1982; **55**: 305–10.
6 Steinberg ML, Defendi V. Transformation and immortalization of human keratinocytes by SV40. *J Invest Dermatol* 1983; **81**: 131–6.
7 Smogorzewska A, de Lange T. Different telomere damage signaling pathways in human and mouse cells. *EMBO J* 2002; **21**: 4338–48.
8 Bodnar AG, Ouellette M, Frolkis M *et al.* Extension of life-span by introduction of telomerase into normal human cells. *Science* 1998; **279**: 349–52.
9 Terai M, Uyama T, Sugiki T, Li XK, Umezawa A, Kiyono T. Immortalization of human fetal cells: The life span of umbilical cord blood-derived cells can be prolonged without manipulating p16INK4a/RB braking pathway. *Mol Biol Cell* 2005; **16**: 1491–9.
10 Kiyono T, Foster SA, Koop JI, McDougall JK, Galloway DA, Klingelhutz AJ. Both Rb/p16INK4a inactivation and telomerase activity are required to immortalize human epithelial cells. *Nature* 1998; **396**: 84–8.
11 Veldman T, Liu X, Yuan H, Schlegel R. Human papillomavirus E6 and Myc proteins associate in vivo and bind to and cooperatively activate the telomerase reverse transcriptase promoter. *Proc Natl Acad Sci USA* 2003; **100**: 8211–16.
12 Gewin L, Myers H, Kiyono T, Galloway DA. Identification of a novel telomerase repressor that interacts with the human papillomavirus type-16, E6/E6–AP complex. *Genes Dev* 2004; **18**: 2269–82.
13 Okamoto T, Aoyama T, Nakayama T *et al.* Clonal heterogeneity in differentiation potential of immortalized human mesenchymal stem cells. *Biochem Biophys Res Commun* 2002; **295**: 354–61.
14 Kyo S, Nakamura M, Kiyono T *et al.* Successful immortalization of endometrial glandular cells with normal structural and functional characteristics. *Am J Pathol* 2003; **163**: 2259–69.
15 Ahuja D, Saenz-Robles MT, Pipas JM. SV40 large T antigen targets multiple cellular pathways to elicit cellular transformation. *Oncogene* 2005; **24**: 7729–45.
16 Sugimoto M, Tahara H, Ide T, Furuichi Y. Steps involved in immortalization and tumorigenesis in human B-lymphoblastoid cell lines transformed by Epstein-Barr virus. *Cancer Res* 2004; **64**: 3361–4.
17 Cohen JI, Wang F, Kieff E. Epstein-Barr virus nuclear protein 2 mutations define essential domains for transformation and transactivation. *J Virol* 1991; **65**: 2545–54.
18 Hammerschmidt W, Sugden B. Genetic analysis of immortalizing functions of Epstein-Barr virus in human B lymphocytes. *Nature* 1989; **340**: 393–7.
19 Kaye KM, Izumi KM, Kieff E. Epstein-Barr virus latent membrane protein 1 is essential for B-lymphocyte growth transformation. *Proc Natl Acad Sci USA* 1993; **90**: 9150–54.
20 Tomkinson B, Robertson E, Kieff E. Epstein-Barr virus nuclear proteins EBNA-3A and EBNA-3C are essential for B-lymphocyte growth transformation. *J Virol* 1993; **67**: 2014–25.
21 Humme S, Reisbach G, Feederle R *et al.* The EBV nuclear antigen 1 (EBNA1) enhances B cell immortalization several thousandfold. *Proc Natl Acad Sci USA* 2003; **100**: 10 989–94.
22 Masutomi K, Yu EY, Khurts S *et al.* Telomerase maintains telomere structure in normal human cells. *Cell* 2003; **114**: 241–53.
23 Liu K, Schoonmaker MM, Levine BL, June CH, Hodes RJ, Weng NP. Constitutive and regulated expression of telomerase reverse transcriptase (hTERT) in human lymphocytes. *Proc Natl Acad Sci USA* 1999; **96**: 5147–52.
24 Weng NP, Granger L, Hodes RJ. Telomere lengthening and telomerase activation during human B cell differentiation. *Proc Natl Acad Sci USA* 1997; **94**: 10 827–32.
25 Hu BT, Lee SC, Marin E, Ryan DH, Insel RA. Telomerase is up-regulated in human germinal center B cells in vivo and can be re-expressed in memory B cells activated in vitro. *J Immunol* 1997; **159**: 1068–71.
26 Schultze JL, Cardoso AA, Freeman GJ *et al.* Follicular lymphomas can be induced to present alloantigen efficiently: A conceptual model to improve their tumor immunogenicity. *Proc Natl Acad Sci USA* 1995; **92**: 8200–4.
27 Kondo E, Topp MS, Kiem HP *et al.* Efficient generation of antigen-specific cytotoxic T cells using retrovirally transduced CD40-activated B cells. *J Immunol* 2002; **169**: 2164–71.
28 Smotkin D, Prokoph H, Wettstein FO. Oncogenic and nononcogenic human genital papillomaviruses generate the E7 mRNA by different mechanisms. *J Virol* 1989; **63**: 1441–7.
29 Naviaux RK, Costanzi E, Haas M, Verma IM. The pCL vector system: Rapid production of helper-free, high-titer, recombinant retroviruses. *J Virol* 1996; **70**: 5701–5.
30 Miller AD, Garcia JV, von Suhr N, Lynch CM, Wilson C, Eiden MV. Construction and properties of retrovirus packaging cells based on gibbon ape leukemia virus. *J Virol* 1991; **65**: 2220–24.
31 Gudjonsson T, Villadsen R, Nielsen HL, Ronnov-Jessen L, Bissell MJ, Petersen OW. Isolation, immortalization, and characterization of a human breast epithelial cell line with stem cell properties. *Genes Dev* 2002; **16**: 693–706.
32 Foster SA, Wong DJ, Barrett MT, Galloway DA. Inactivation of p16 in human mammary epithelial cells by CpG island methylation. *Mol Cell Biol* 1998; **18**: 1793–801.
33 Alcorta DA, Xiong Y, Phelps D, Hannon G, Beach D, Barrett JC. Involvement of the cyclin-dependent kinase inhibitor p16 (INK4a) in replicative senescence of normal human fibroblasts. *Proc Natl Acad Sci USA* 1996; **93**: 13 742–7.
34 Erickson S, Sangfelt O, Heyman M, Castro J, Einhorn S, Grander D. Involvement of the Ink4 proteins p16 and p15 in T-lymphocyte senescence. *Oncogene* 1998; **17**: 595–602.
35 Herbert BS, Wright WE, Shay JW. p16 (INK4a) inactivation is not required to immortalize human mammary epithelial cells. *Oncogene* 2002; **21**: 7897–900.
36 Rheinwald JG, Hahn WC, Ramsey MR *et al.* A two-stage, p16 (INK4A)- and p53-dependent keratinocyte senescence mechanism that limits replicative potential independent of telomere status. *Mol Cell Biol* 2002; **22**: 5157–72.
37 Igarashi H, Sakaguchi N. Telomerase activity is induced in human peripheral B lymphocytes by the stimulation to antigen receptor. *Blood* 1997; **89**: 1299–307.
38 Jung D, Neron S, Lemieux R, Roy A, Richard M. Telomere-independent reduction of human B lymphocyte: Proliferation during long-term culture. *Immunol Invest* 2001; **30**: 157–68.
39 Klingelhutz AJ, Foster SA, McDougall JK. Telomerase activation by the E6 gene product of human papillomavirus type 16. *Nature* 1996; **380**: 79–82.
40 Scheffner M, Werness BA, Huibregtse JM, Levine AJ, Howley PM. The E6 oncoprotein encoded by human papillomavirus types 16 and 18 promotes the degradation of p53. *Cell* 1990; **63**: 1129–36.
41 Imadome K, Shirakata M, Shimizu N, Nonoyama S, Yamanashi Y. CD40 ligand is a critical effector of Epstein-Barr virus in host cell survival and transformation. *Proc Natl Acad Sci USA* 2003; **100**: 7836–40.
42 Yatabe Y, Oka K, Asai J, Mori N. Poor correlation between clonal immunoglobulin gene rearrangement and immunoglobulin gene transcription in Hodgkin's disease. *Am J Pathol* 1996; **149**: 1351–61.
43 Akimov SS, Ramezani A, Hawley TS, Hawley RG. Bypass of senescence, immortalization, and transformation of human hematopoietic progenitor cells. *Stem Cells* 2005; **9**: 1423–33.
44 Ohtani N, Brennan P, Gaubatz S *et al.* Epstein-Barr virus LMP1 blocks p16INK4a-RB pathway by promoting nuclear export of E2F4/5. *J Cell Biol* 2003; **162**: 173–83.

JOURNAL OF BIOSCIENCE AND BIOENGINEERING
Vol. 102, No. 5, 467–469. 2006
DOI: 10.1263/jbb.102.467



# *Ex Vivo* Expansion of Human Cord Blood Hematopoietic Progenitor Cells Using Glutaraldehyde-Fixed Human Bone Marrow Stromal Cells

Yoshihiro Ito,[1,2]* Hirokazu Hasauda,[1] Takashi Kitajima,[1] and Toru Kiyono[3]

*Regenerative Medical Bioreactor Project, Kanagawa Academy of Science and Technology, KSP East 309, 3-2-1 Sakado, Takatsu-ku, Kawasaki, Kanagawa 213-0012, Japan,[1] Nano Medical Engineering Laboratory, RIKEN (The Institute of Physical and Chemical Research), 2-1 Hirosawa, Wako 351-0198, Japan,[2] and Virology Division, Research Institute, National Cancer Center, 5-1-1 Tsukiji, Chuo-ku, Tokyo 104-0045, Japan[3]*

Received 20 July 2006/Accepted 8 August 2006

**Human stromal cells were immortalized and fixed with glutaraldehyde to support an *ex vivo* expansion of human cord blood hematopoietic progenitor cells. In addition, this enabled glutaraldehyde-fixed stromal cells to be stored at 4°C. Although freeze-dried glutaraldehyde-fixed stromal cells did not increase the number of the progenitor cells, the percent decrease in the number of $CD34^+$ cells in the presence of freeze-dried glutaraldehyde-fixed stromal cells was less than that in the absence of the stromal cells. Thus, glutaraldehyde-fixed stromal cells can serve as a stabilizing device for hematopoietic cell expansion.**

[**Key words:** hematopoietic cells, *ex vivo* expansion, glutaraldehyde fixation, stromal cell, cord blood cells]

Human umbilical cord blood (CB) is an attractive source of cells for transplantation therapy and regenerative medicine because it contains hematopoietic progenitor and stem cells, is relatively immature in terms of immune responsiveness, and is easy to obtain from CB banks. However, it offers a limited number of cells for widespread medical applications. Many researchers have explored *ex vivo* expansion methods to increase the number of hematopoietic cells (1). A successful expansion of CB cells using hematopoietic growth factors or artificial substrata has been reported by several groups (2–6); however, the expansion efficiency is low in these systems. In contrast, since the establishment of Dexter-type long-term bone marrow (BM) culture (7), which attempts to mimic the BM environment, many coculture systems have been reported as promising systems for the maintenance and expansion of hematopoietic progenitor cells (8–10). However, because these systems mainly used murine cell lines and stromal media supplemented with calf and horse sera, they have been considered as sources of xenotransplantation for human hematopoietic cell expansion. Therefore, to reduce the risks of infectious disease, a culture system without the use of animal-derived stromal cells is desirable.

It has recently been reported that the number of human CB cells could be markedly increased in the presence of stem cell factor (SCF), thrombopoietin (TPO), and Flk-2/Flt-3 ligand (FL) by coculture with primary (11) or immortalized (12) human BM stromal cells. Although these techniques are useful, for the primary human CB cells, the use of the patient's own stromal cells is desirable so as not to induce undesirable immunoresponses. Furthermore, for the immortalized human BM stromal cells, contamination with undesirable genes or viral vectors must be considered. In addition, the preparation of stromal cells for each expansion is troublesome. Therefore, in this investigation, we prepared chemically fixed stromal cells, which can be cool-stored, for the expansion of human CB hematopoietic cells.

First, we constructed the retroviral plasmids pCMSCVpuro-16E6E7 and pCLXSN-hTERT as described previously (13) to prepare an immortalized stromal cell for a stable supply. The production of recombinant retroviruses has been described previously (13, 14). Briefly, the retroviral vector plasmids were cotransfected with pCL-10A1, which is a packaging construct encoding gag, pol, and env of the murine leukemia virus strain 10A1, into 293FT cells (Invitrogen, Carlsbad, CA, USA) using TransIT-293 (Mirus, Madison, WI, USA), in accordance with the manufacturer's instructions, and the culture fluid was harvested at 48 to 72 h post-transfection. The retrovirus, MSCVpuro-16E6E7 contains the human papillomavirus type 16 (HPV-16) genes E6 and E7, which inhibit p53 and Rb, respectively, and a puromycin resistance gene. The LXSN-hTERT retrovirus expresses the catalytic subunit of human telomerase reverse transcriptase, which inhibits the shortening of telomeres, and a neomycin (G418) resistance gene. The titer of recombinant retroviruses was greater than $3\times10^5$ drug-resistant colony forming units per milliliter in HeLa cells.

Second-passage primary human BM stromal cells (human mesenchymal stem cells, cat no. PT-2501, lot no. 3F0664)

* Corresponding author. e-mail: y-ito@ksp.or.jp
phone: +81-(0)44-819-2044 fax: +81-(0)44-819-2039

TABLE 1. Total number of human CB progenitor cells[a] after culture[b]

| Lot no. | Stroma free ($\times 10^4$ cells) | GA-fixed stroma ($\times 10^4$ cells) | GA-fixed stroma/Stroma-free | Culture time (d) | n |
|---|---|---|---|---|---|
| 1 | 28.0±1.8 | 58.0±13.5 | 2.1 | 14 | 6 |
| 2 | 17.7±1.5 | 24.2±3.3 | 1.4 | 14 | 6 |
| 3 | 74.0±9.8 | 123.3±22.5 | 1.7 | 14 | 6 |
| 4 | 275.8±30.4 | 395.8±30.1 | 1.4 | 14 | 6 |
| 5 | 35.7±4.4 | 62.5±10.0 | 1.8 | 14 | 6 |
| 6 | 114.0±18.8 | 188.7±25.8 | 1.7 | 14 | 6 |
| 7 | 31.0±5.7 | 76.5±6.0 | 2.5 | 14 | 6 |
| 8 | 57.2±3.5 | 85.5±2.9 | 1.5 | 10 | 6 |
| 9 | 115.3±10.5 | 189.4±24.3 | 1.6 | 10 | 6 |
| 10 | 27.3±2.6 | 46.2±5.8 | 1.7 | 10 | 6 |

[a] CB samples were obtained from the RIKEN BioResource Center (Tsukuba). CB mononuclear cells were washed with PBS containing 10% acid citrate dextrose-A, (ACD-A; Terumo, Tokyo) and 500 ml of 10% BSA (Sigma, St. Louis, MO, USA). $CD34^-$ cell-enriched populations were separated from mononuclear cells with a MACS Direct CD34 Progenitor Cell Isolation kit (Miltenyi Biotec, Bergisch-Gladbach, Germany) following the manufacturer's instructions.

[b] Ten thousand $CD34^+$ cells were cultured on stromal cell layers in 1 ml of minimum essential medium α (α-MEM) supplemented with 20% fetal bovine serum (FBS), human SCF (10 ng/ml), human TPO (10 ng/ml), and human FL (10 ng/ml). Ideally, the addition of no serum was desired for the expansion; however, in this study, serum was added to the medium because it can be easily replaced with patient sera in the future. The culture was maintained at 37°C in a humidified atmosphere of 5% $CO_2$/95% air. After one week of culture, 1 ml of fresh medium was added and the coculture was continued for another week. At the end of the culture period, hematopoietic cells that did not adhere to stromal cells and those that adhered only weakly to stromal cells were collected by gentle pipetting.

TABLE 2. Total number and percentage of $CD34^+$ cells[a] of human CB progenitor cells cultured under same conditions as those described in Table 1 during 10 d

| | Stroma-free | GA-fixed stroma | GA-fixed/freeze-dried stroma | n |
|---|---|---|---|---|
| Total number of cells ($\times 10^4$) | 115.3±10.5 | 189.4±24.4 | 119.3±8.8 | 6 |
| Percentage of $CD34^+$ cells (%) | 4.6±0.1 | 7.0±0.1 | 8.0±0.4 | 3 |

[a] Cell suspensions were incubated with the fluorescein isothiocyanate-conjugated anti-CD34 antibody and the phycoerythrin-conjugated anti-CD45 antibody (Beckman Coulter, Tokyo) in PBS/5% FBS at room temperature for 10 min. The analysis was carried out using a Cytomics FC500 flow cytometer (Beckman Coulter). Dead cells were gated out with a forward versus side scatter window by 7-amino-actinomycin D staining.

were purchased from Cambrex (East Rutherford, NJ, USA) and the cells were maintained in mesenchymal stem cell growth medium (MSCGM, Cambrex, cat. no. PT-3001). Two days after $5 \times 10^4$ cells were plated on 35 mm-well of a six-well plate, 1 ml of the retrovirus culture fluid was added to each well in the presence of polybrene (4 μg/ml). Cells were first inoculated with LXSN-hTERT, and the infected cells were selected in the presence of 800 μg/ml G418. Then, the cells were inoculated with MSCVpuro-16E6E7, followed by selection in the presence of 0.4 μg/ml puromycin. Because the cells not transduced with E6 and E7 genes underwent premature senescence within a few passages, the cells with an extended lifespan were used as virtually immortal stromal cells. One hundred thousand stromal cells were plated in six-well plates and cultured for 6–7 d. The cultured stromal cells were fixed with 2.5% glutaraldehyde in phosphate buffered saline (PBS) for 30 min, following extensive washing with PBS. The prepared cells were stored for further experiments in PBS at 4°C. Freeze-drying was performed after washing with water, and the freeze-dried cells were stored for further experiments in air at room temperature.

The immortalized cells were prepared by the same method as that previously reported (15, 16) and considered to have similar properties. When compared with that of the cells established by Kawano *et al.* (12), the growth rate of the cells in our study was significantly high; it was difficult to decrease the growth rate using mitomycin C. Next, the cells were directly chemically fixed. Cells treated with glutaraldehyde had almost the same morphology as nontreated cells. Furthermore, glutaraldehyde-treated stromal cell layers maintained their morphology even after four weeks in a refrigerator, although they formed small interstitial spaces. Freeze-drying also did not affect the morphology.

We examined the ability of the fixed stromal cells to support hematopoiesis (Table 1). Ten thousand human CB $CD34^+$ cells were cultured in serum-containing medium supplemented with SCF, TPO, and FL. It was considered that cell viability differed among the CB preparations because the CB collected by the RIKEN Bioresource Center was obtained from various hospitals under different conditions. However, compared with stromal cell-free culture, glutaraldehyde-fixed stromal cell cuture increased the number of cells 1.7-fold over 10 d or two weeks, although the absolute number of cells significantly depended on the sample lot. We concluded that stromal cell layers clearly retained the ability to enhance CB cell expansion even after glutaraldehyde fixation.

Table 2 shows that the percentage of $CD34^+$ cells was greater in glutaraldehyde-fixed stromal cell culture than in stromal cell-free culture. In addition, in contrast with the glutaraldehyde-fixed stromal cells, the freeze-dried glutaraldehyde-fixed stromal cells did not support the expansion of human CB progenitor cells; however, they did not decrease

the percentage of $CD34^+$ cells, whereas the glutaraldehyde-fixed stromal cells did.

For clinical applications, the expansion system requires safety, reproducibility, and a stable source of cultured cells. To fulfill these requirements, it is desirable for the system not to use viable cells. Our results revealed that a substrate can be used as an expansion device instead of living cells. If bioactive molecules are extracted with their bioactivity preserved, a proper rearrangement on the matrix will provide a new useful expansion device. We previously attempted to immobilize bioactive molecules on a solid matrix by photoimmobilization and showed the effectiveness of this approach for cell expansion (17). The present method could also be useful for creating a cell expansion system.

In conclusion, glutaraldehyde-fixed stromal cells retain the ability to support hematopoiesis via the *ex vivo* expansion of human CB progenitor cells through a direct interaction between the hematopoietic cells and the fixed stromal cell surface, and this ability is maintained after simple refrigeration at 4°C.

This work was partially supported by a Grant-in-Aid for Scientific Research from the Ministry of Education, Culture, Sports, Science and Technology of Japan (no. 14380406) and the Uehara Memorial Foundation.

## REFERENCES

1. **Heike, T. and Nakahata, T.:** *Ex vivo* expansion of hematopoietic stem cells by cytokines. Biochim. Biophys. Acta, **1592**, 313–321 (2002).
2. **Piacibello, W., Sanavio, F., Severino, A., Dane, A., Gammaitoni, L., Fagioli, F., Perissinotto, E., Cavalloni, G., Kollet, O., Lapidot, T., and Aglietta, M.:** Engraftment in nonobese diabetic severe combined immunodeficient mice of human CD34(+) cord blood cells after *ex vivo* expansion: evidence for the amplification and self-renewal of repopulating stem cells. Blood, **93**, 3736–3749 (1999).
3. **Bhatia, M., Bonnet, D., Kapp, U., Wang, J. C., Murdoch, B., and Dick, J. E.:** Quantitative analysis reveals expansion of human hematopoietic repopulating cells after short-term ex vivo culture. J. Exp. Med., **186**, 619–624 (1997).
4. **Glimm, H., Oh, I. H., and Eaves, C. J.:** Human hematopoietic stem cells stimulated to proliferate *in vitro* lose engraftment potential during their S/G(2)/M transit and do not reenter G(0). Blood, **96**, 4185–4193 (2000).
5. **Takagi, M.:** Cell processing engineering for *ex-vivo* expansion of hematopoietic cells. J. Biosci. Bioeng., **99**, 189–196 (2004).
6. **Jiang, X. S., Chai, C., Zhang, Y., Zhuo, R. X., Mao, H. Q., and Leong, K. W.:** Surface-immobilization of adhesion peptides on substrate for *ex vivo* expansion of cryopreserved umbilical cord blood $CD34^+$ cells. Biomaterials, **27**, 2723–2732 (2006).
7. **Dexter, T. M., Allen, T. D., Lajtha, L. G., Schofield, R., and Lord, B. I.:** Stimulation of differentiation and proliferation of haemopoietic cells *in vitro*. J. Cell Physiol., **82**, 461–473 (1973).
8. **Kanai, M., Hirayama, F., Yamaguchi, M., Ohkawara, J., Sato, N., Fukazawa, K., Yamashita, K., Kuwabara, M., Ikeda, H., and Ikebuchi, K.:** Stromal cell-dependent *ex vivo* expansion of human cord blood progenitors and augmentation of transplantable stem cell activity. Bone Marrow Transplant., **26**, 837–844 (2000).
9. **Xu, M. J., Tsuji, K., Ueda, T., Mukouyama, Y. S., Hara, T., Yang, F. C., Ebihara, Y., Matsuoka, S., Manabe, A., Kikuchi, A., Ito, M., Miyajima, A., and Nakahata, T.:** Stimulation of mouse and human primitive hematopoiesis by murine embryonic aorta-gonad-mesonephros-derived stromal cell lines. Blood, **92**, 2032–2040 (1998).
10. **Moore, K. A., Ema, H., and Lemischka, I. R.:** *In vitro* maintenance of highly purified, transplantable hematopoietic stem cells. Blood, **89**, 4337–4347 (1997).
11. **Yamaguchi, M., Hirayama, F., Kanai, M., Sato, N., Fukazawa, K., Yamashita, K., Sawada, K., Koike, T., Kuwabara, M., Ikeda, H., and Ikebuchi, K.:** Serum-free coculture system for *ex vivo* expansion of human cord blood primitive progenitors and SCID mouse-reconstituting cells using human bone marrow primary stromal cells. Exp. Hematol., **29**, 174–182 (2001).
12. **Kawano, Y., Kobune, M., Yamaguchi, M., Nakamura, K., Ito, Y., Sasaki, K., Takahashi, S., Nakamura, T., Chiba, H., Sato, T., and other 7 authors:** *Ex vivo* expansion of human umbilical cord hematopoietic progenitor cells using a coculture system with human telomerase catalytic subunit (hTERT)-transfected human stromal cells. Blood, **101**, 532–540 (2003).
13. **Kyo, S., Nakamura, M., Kiyono, T., Maida, Y., Kanaya, T., Tanaka, M., Yatabe, N., and Inoue, M.:** Successful immortalization of endometrial glandular cells with normal structural and functional characteristics. Am. J. Pathol., **163**, 2259–2269 (2003).
14. **Imabayashi, H., Mori, T., Gojo, S., Kiyono, T., Sugiyama, T., Irie, R., Isogai, T., Hata, J., Toyama, Y., and Umezawa, A.:** Redifferentiation of dedifferentiated chondrocytes and chondrogenesis of human bone marrow stromal cells via chondrosphere formation with expression profiling by large-scale cDNA analysis. Exp. Cell Res., **288**, 35–50 (2003).
15. **Takeda, Y., Mori, T., Imabayashi, H., Kiyono, T., Gojo, S., Miyoshi, S., Hida, N., Ita, M., Segawa, K., Ogawa, S., Sakamoto, M., Nakamura, S., and Umezawa, A.:** Can the life span of human marrow stromal cells be prolonged by bmi-1, E6, E7, and/or telomerase without affecting cardiomyogenic differentiation? J. Gene Med., **6**, 833–845 (2004).
16. **Mori, T., Kiyono, T., Imabayashi, H., Takeda, Y., Tsuchiya, K., Miyoshi, S., Makino, H., Matsumoto, K., Saito, H., Ogawa, S., Sakamoto, M., Hata, J., and Umezawa, A.:** Combination of hTERT and bmi-1, E6, or E7 induces prolongation of the life span of bone marrow stromal cells from an elderly donor without affecting their neurogenic potential. Mol. Cell Biol., **25**, 5183–5195 (2005).
17. **Ito, Y., Hasuda, H., Yamauchi, T., Komatsu, N., and Ikebuchi, K.:** Immobilization of erythropoietin to culture erythropoietin-dependent human leukemia cell line. Biomaterials, **25**, 2293–2298 (2004).

Biochemical Journal Immediate Publication. Published on 13 Mar 2007 as manuscript BJ20070104

# Runx3 Negatively Regulates Osterix Expression in Dental Pulp Cells

Li Zheng[†], Koichiro Iohara[†], Masaki Ishikawa[‡], Takeshi Into[†], Teruko Takano-Yamamoto[§], Kenji Matsushita[†], Misako Nakashima[†*]

[†]*Laboratory of Oral Disease Research, National Institute for Longevity Sciences, National Center for Geriatrics and Gerontology, Aichi 474-8522, JAPAN*

[‡]*Department of Endodontology and Operative Dentistry, Division of Oral Rehabilitation, Faculty of Dental Science, Kyushu University, Fukuoka 812-8582, JAPAN*

[§]*Division of Orthodontics and Dentofacial Orthopedics, Graduate School of Dentistry, Tohoku University, Sendai 980-8575, JAPAN*

[*]Address correspondence to this author at

Laboratory of Oral Disease Research,
National Institute for Longevity Sciences,
National Center for Geriatrics and Gerontology,
36-3 Gengo, Morioka, Obu, Aichi 474-8522, JAPAN
Phone: 81-562-44-5651 ext. 5063, FAX: 81-562-46-8684
E-mail: misako@nils.go.jp

**Synopsis**

Osterix, a zinc finger-containing transcription factor, is required for osteoblast differentiation and bone formation. *Osterix* is also expressed in dental mesenchymal cells of the tooth germ. However, the transcritional regulation by osterix of tooth development is not clear. Genetic studies in osteogenesis place *Osterix* downstream to *Runx2*. *Osterix* was expressed in odontoblasts, overlapping with *Runx3* during their terminal differentiation in vivo. Runx3 down-regulated *Osterix* expression in the mouse dental pulp cells. Therefore, the regulatory role of Runx3 on *Osterix* expression in tooth development was investigated. Enforced expression of *Runx3* down-regulated the *Osterix* promoter activity in a cell line HEK293. When the Runx3 responsive element on the *Osterix* promoter, -713 bp to -707 bp (site 3, AGTGGTT) from the cap site, was mutated, this down-regulation was abrogated. Furthermore,

electrophoretic mobility-shift assay (EMSA) and Chromatin immunoprecipitation (ChIP) assays in the mouse dental pulp cells demonstrated direct functional binding of Runx3 to *Osterix* promoter. These results demonstrate the transcriptional regulation of *Osterix* expression by Runx3 during differentiation of dental pulp cells into odontoblasts in tooth development.

**Short Title:** Down-regulation of *Osterix* by Runx3

**Keywords:** Dental pulp cells, Runx3, Runx2, Osterix, Bone morphogenetic protein 2, tooth development

**Abbreviations footnote:** BMP, bone morphogenetic protein, RT-PCR, reverse transcription-polymerase chain reaction, Dspp, Dentin sialophosphoprotein, KLK4, Kallikrein 4, DPCs, dental pulp cells

## INTRODUCTION

The transcriptional regulation of cell proliferation and differentiation by the Runt-related (RUNX) family of DNA-binding transcription factors is critical for both morphogenesis and regeneration. The regulatory function of Runx family on the promoters and enhancers of target genes where they associate with cofactors and other DNA-binding transcription factors to modulate gene expression is well known [1]. Runx family is composed of three members of Runx family designated Runx1/AML1/Cbfa2, Runx2/AML2/Cbfa1, Runx3/AML3/Cbfa3 [2, 3]. Although the Runx members share highly conserved DNA binding domains, they regulate distinct functions [4-7]. Runx1 is involved in regulation of hematopoiesis[8]. Runx2 are essential for bone and tooth development [9-11]. Runx3 is critical for gastric epithelial differentiation, neurogenesis of the dorsal root ganglia and T cell differentiation[8-10, 12-16].

Stringent control of gene activation and suppression is required for tooth development. The optimal gene expression during dentin formation is dependent on

integration and regulation of signals that governs the commitment of stem/progenitor cells to pulp cell lineage and proliferation and differentiation into odontoblasts. Runx2 is essential for tooth formation. Molar development is arrested at the late bud stage in Runx2 homozygous mice [11], correlating with the intense expression of Runx2 in the dental mesenchyme during the bud and cap stages [17]. Runx3 is coexpressed in dental papilla at the cap and early bell stages with Runx2. Later Runx3 is restricted to the odontoblastic layer at the late bell stage while Runx2 is no longer detected [17]. Runx proteins might play a pivotal role in governing physiologically responsive control of dental genes.

Osterix, a zinc finger-containing transcription factor, is required for osteoblast differentiation and bone formation [18]. In *Osterix* null mice, no bone formation occurs, similar to the phenotypes in *Runx2* null mice [9, 18]. However, Runx2 is expressed without major alterations in *Osterix* null mice. In contrast, *Osterix* is not expressed in Runx2 null mice, demonstrating that Osterix acts downstream of Runx2 [18]. Recently transcriptional regulation of *Osterix* in cartilage by Runx2 has been suggested [19]. *Osterix* is expressed in mesenchymal cells of the tooth germ [18]. The expression of *Osterix* and its transcriptional regulation by Runx during tooth development have not been investigated.

In the present study, we investigated the expression of *Osterix* during tooth development, and demonstrated that *Osterix* was strictly expressed in odontoblastic layer at the bell and the differentiation stage, overlapping with *Runx3*. Therefore, the regulation of the expression of *Osterix* by Runx3 was further examined. Our results demonstrated that Runx3 directly binds to *Osterix* promoter and down regulates its expression in dental pulp cells.

## EXPERIMENTAL

### *Cloning of the Osterix promoter*

To clone the Osx promoter (nucleotide 66 to 1751; GenBank accession no. DQ229136), genomic DNA was isolated from the tail of ICR mouse. PCR was performed using two primers, Osterix promoter 5'-1:

5'-TCTGTCCCTCAGTCCTGCTT-3'; Osterix promoter 3'-2: 5-GGGCAAGTTGTCAGAGCTTC-3'. The 1.7 kb PCR product was then subcloned into *MluI*/*Xho*I site of pGL3-promoter vector (Promega, Madison, WI, U.S.A.), named pOsx1.7-luc. To prepare the *MSCV-eGFP-Flag-Runx3* expression vector, following primers were used: Flag-Runx3-5': 5'-GGCAGATCTGCCACCATGGACTACAAGGACGATGACGACAAGGCTTCC AACAGCATCTTTG-3' and Flag-Runx3-3': 5'-ATATGAGCTCTCCCGCGTGGT-3' to generate a Runx3 fragment with FLAG motif at N-terminal. The 300 bp PCR product was cloned into the *Bgl*II-*Sac*I site in PSL1180 vector (GE Healthcare, Buckinghamshire, U.K.) and named Flag-Runx3-300bp-PSL1180. A 1.0 kb Runx3 fragment was digested with *Sac*I from *MSCV-eGFP-Runx3* plasmid (kindly provided by Dr. Taniuchi Ichiro, Laboratory of Transcriptional Regulation, RIKEN Research Center for Allergy and Immunology, Yokohama, Japan) and subcloned into Flag-Runx3-300bp-PSL1180 vector, named Flag-Runx3-PSL1180. The 1.3 kb full length of Runx3 with Flag-tagged N-terminal was digested with *Bgl*II from Flag-Runx3-PSL1180 and subcloned into *MSCV-eGFP* vector, named with *MSCV-eGFP-Flag-Runx3*. The orientation of the inserts was confirmed by sequencing.

*Site-directed mutagenesis*

Three putative Runx2-binding sequence -1823 to -1817, -1776 to -1771 and -713 to -707 bp from the Cap site [19] were mutated using the QuickChange Site-Directed Mutagenesis Kit (Stratagene, La Jolla, CA, U.S.A.) according to the manufacturer's recommendations. We generated mutants as follows; 5'-AACCACA-3' at -1823/-1817 bp was changed into 5'-**GAGCTCA**-3', 5'-ACCACT-3' at -1776/-1771 bp was changed into 5'-**GCTACT**-3' and 5'-AGTGGTT-3' at -713/-707 bp was changed into 5'-**ATAGACT**-3'. The mutated nucleotides are indicated in bold. Mutations in single, double, and triple motifs were termed M1-M5 (Fig. 3B). Incorportation of the mutated substitution of all constructs were confirmed by sequencing.

Biochemical Journal Immediate Publication. Published on 13 Mar 2007 as manuscript BJ20070104

*In situ hybridization*

ICR Mouse embryos at 15.0 dpc, 17.0 dpc and postnatal day 1 were fixed in 4 % paraformaldehyde at 4 °C overnight. In situ hybridization was carried out as previously described [20]. Primers (Osterix-5'-1: 5'-GGTCCAGGCAACACACCTAC-3'; Osterix-3'-2: 5'-GGTAGGGAGCTGGGTTAAGG-3') were used to amplify the mouse *Osterix* cDNA. PCR product was ligated into pBluescript II SK (-) vector (Stratagene). Mouse *Runx3* cDNA was digested by *EcoR*I from mouse *MSCV-eGFP-Runx3* plasmid, then subcloned into pBluescript II SK (-) vector. All inserts were confirmed by sequencing. The following cDNAs were used to generate sense and antisense riboprobes using either T3 or T7 RNA polymerase: a 184 bp murine Osterix fragment, a 1.2 kb Runx3 fragment and a 1.2 kb Bmp2 fragment. In situ hybridization was performed as described previously [21]

*Cell Culture and transfection studies*

Mouse dental pulp cells (DPCs) were isolated from tooth germ at 17.0 dpc. mDPC and HEK293 cells (epithelial cell line derived from human kidney transformed embryonic cells) were maintained in Dulbecco's modified Eagle's medium (DMEM) (Sigma, St. Louis, MO, U.S.A.) supplemented with 100 units/ml penicillin G, 100 μg/ml streptomycin (Invitrogen, Carlsbad, CA, U.S.A.) and 10% (v/v) fetal bovine serum (SAFC Biosciences, Lenexa, Kansas, U.S.A.). Experiments assessing promoter activity by luciferase were performed as follows. HEK293 cells ($1x10^5$) were plated in 24-well plates in antibiotics-free and serum-free DMEM one day before, and transiently transfected with 2 μg of each promoter/pGL3 luciferase reporter plasmids, 3 μg of expression plasmid, and 0.2 μg of SV-40 promoter construct (Promega) as an internal standardize control for transfection efficiency. Transfections were performed using 2 μl/well of Lipofectamine 2000 (Invitrogen) following the manufacturer's instructions. *MSCV-eGFP* plasmid was also transfected as control. After 4 h, the medium was changed into DMEM with 10% (v/v) foetal bovine serum and cultured

for an additional 44 h. Cells were then lysed, and luciferase activity was determined using a Dual Luciferase Report Assay kit as instructed by the manufacturer (Promega). All activities were normalized against co-transfected internal control plasmid pRL-SV40 (Promega). For overexpression experiments, 4 x $10^6$ DPCs were transfected by 8 μg of expression plasmid using ECM 830 Electroporator (BTX, San Diego, CA, U.S.A.) following the manufacturer's instructions, then plated on collagen type I-coated 35 mm dish (Iwaki, Chiba, Japan). After 4 h, the medium was changed into DMEM with 10% (v/v) foetal bovine serum. Cells were harvested at 0h, 24h, and 48h after transfection. The cell viability was determined with trypan blue soon after transfection, and the efficiency was estimated by fluorescent microscopy 24 hours after transfection with the plasmid vector *AFP* (kindly provided by Dr. Hidesato Ogawa, Graduate School of Biological Sciences, Nara Institute of Science and Technology, Japan).

*Real time reverse transcriptase polymerase-chain reaction (RT-PCR) analysis*

Total RNA was extracted by using Trizol (Invitrogen), and 2 μg of freshly isolated RNA was reverse transcribed with SuperScript II Reverse Transcriptase (Invitrogen) following the manufacturer's recommendations. The resulting cDNA was then amplified by Real Time RT-PCR with Light Cycler-FastStart DNA master SYBR Green I (Roche Diagnostics, Mannheim, Germany). The primers used in this study are presented in Table 1.

*Preparation of nuclear extracts*

Nuclear extract was isolated as previously reported [22]. Briefly, mouse DPCs was washed with 10 ml of PBS, scraped in 1.5 ml ice cold PBS, and centrifuged at 100 ***g*** for 5 min. The pellet was suspended in 1 ml of PBS and centrifuged again at 660 ***g*** for 15 sec. After resuspension in cold buffer A (10 mM Hepes, pH 7.9, 10 mM KCl, 0.1 mM EDTA, 0.1 mM EGTA, 1mM dithiothreitol and 0.5 mM PMSF) on ice for 15 min. The cell membranes were lysed by Nonidet P40 at a final concentration of 0.5 %, centrifuged at 660 ***g*** for 30 sec, and the pelleted nuclei were resuspended in

cold buffer C (20 mM Hepes, pH 7.9, 0.4 M NaCl, 1mM EDTA, 1 mM EGTA, 1 mM dithiothreitol and 1 mM PMSF). The nuclear protein was extracted by shaking at 4 °C for 15 min, centrifuged at 15,000 ***g*** for 5 min, and the supernatant fractions were collected. The protein content of the nuclear extracts was determined using the Bradford protein analysis method [23].

*Electrophoretic mobility shift assay (EMSA)*

Individual oligonucleotides were annealed to equimolar amounts of their complementary strands (Wild type, Osterix-gel-WT-5'-1: 5'-CAGATCTCTAATTAGTGGTTTGGGGTTTGTTCCTTTTC-3' and Osterix-gel-WT-3'-2: 5'-GAAAAGGAACAAACCCCAAACCACTAATTAGAGATCTG-3'; mutant, Osterix-gel-MT-5'-1: 5'-CAGATCTCTAATTATAGACTTGGGGTTTGTTCCTTTTC-3' and Osterix-gel-MT-3'-2: 5'-GAAAAGGAACAAACCCCAAGTCTATAATTAGAGATCTG-3') by heating to 95 °C for 5 min and slowly cooling to room temperature. DIG Gel Shift Kit, 2nd generation (Roche Diagnostics) was used in electrophoretic mobility shift assay according to the manufacturer's protocol. Briefly, wild type double-stranded oligonucleotide probes were labeled with digoxigenin-11-ddUTP at 3'-ends. The labelled probes (20 fmol) were added to 10 μg nuclear extracts in a binding buffer (20 mM Hepes, pH 7.6, 1 mM EDTA, 10 mM $(NH_4)_2SO_4$, 1 mM DTT, 0.2 % (w/v) Tween 20, 30 mM KCl, 25 ng/μl poly d (I-C), 25 ng/μl poly d (A-T) and 50 ng/μl poly L-lysine) at room temperature for 30 min. For competition experiments, 125-fold unlabelled cold oligonucleotides were added in the mixture. After incubation, the protein–DNA complexes were separated by 6% acrylamide native polyacrylamide gel electrophoresis, transferred to a nylon membrane (Whatman Inc., New Jersey, U.S.A.) by contact-blotting, and detected by the DIG-detection kit. Antibody against Runx3 (Active Motif, Carlsbad, CA, U.S.A.) was added to examine specificity of the protein-DNA complex.

*Chromatin immunoprecipitation (ChIP) assay*

Mouse DPCs were treated for 10 min of 1% formaldehyde and washed by ice cold PBS, 3 times, harvested and centrifuged at 100 ***g*** for 5 min. The pellet was suspended in 200 μl of SDS lysis buffer (50 mM Tris-HCl, pH 8.0, 10 mM EDTA, pH 8.0, 1 % (w/v) SDS, 1 mM PMSF, 1 μg/ml aprotinin, 1 μg/ml leupeptin) and incubated on ice for 20 min. The sample was sonicated for 7.5 min (power high, on 30 sec, off 1 min) using a Bioruptor (Cosmo Bio, Tokyo, Japan) to produce soluble chromatin, with average size at 500 bp. The chromatin sample was then diluted nine-fold in ice cold ChIP dilution buffer (50 mM Tris-HCl, pH 8.0, 167 mM NaCl, 1.1 % (v/v) Triton X-100, 0.11 % (w/v) sodium deoxycholate, 1 mM PMSF, 1 μg/ml aprotinin, 1 μg/ml leupeptin). From the diluted sample 200 μl was removed to keep as input fraction at 4 °C. The rest of the sample was precleaned for 6 h using 60 μl of salmon sperm DNA/protein G Sepharose beads at 4 °C, centrifuged at 10,000 ***g*** for 10 sec, and the supernatant was collected. Twenty microgram of rabbit anti-Runx3 polyclonal antibody (Active Motif, Carlsbad, CA, U.S.A.) or 10 μg of goat anti-mouse Runx2 polyclonal antibody (Santa Cruz, CA, U.S.A.) was added and incubated overnight at 4 °C. To collect the immunocomplex, 60 μl of salmon sperm DNA/protein G Sepharose beads were added to the samples for 3 h at 4 °C. The beads were washed once in each of the following buffers, in order: low salt, high salt, and LiCl wash solution; it was then washed twice in TE buffer. The bound protein-DNA immunocomplexes were eluted twice with 200 μl of ChIP direct elution buffer (10 mM Tris-HCl, pH 8.0, 300 mM NaCl, 5 mM EDTA, pH 8.0, 0.5 % (w/v) SDS) and subjected to reverse crosslinking at 65 °C for 6 h. The reverse crosslinked chromatin DNA was further purified by 50 μg/ml proteinase K digestion at 55 °C for 1 h and phenol-chloroform extraction. DNA was then precipitated in ethanol and dissolved in 20 μl of TE buffer. Two microliters of DNA were used for each RT-PCR with primers Osx-ChIP-F: 5'-GAGTGTCGTCCCCAATCC-3' and Osx-ChIP-R: 5'-CTGCTACCACCGAGGCTG-3', yielding a 120-bp product. For a negative control of ChIP assay of Runx3 or Runx2, another $1 \times 10^7$ mouse DPCs was treated as

the same way but with 20 μg rabbit IgG or 10 μg goat IgG. Input (1/20) was used as the positive control of RT-PCR.

*Statistics*

Statistical analyses were performed using Student's unpaired *t*-test. Each experiment was performed at least twice, and the representative data were presented as means ± S.D. of independent replicates ($n \geq 3$).

## RESULTS

*Expression of Runx3, Runx2, Osterix and Bmp2 during tooth development*

In the developing tooth, *Runx3* was detected in the dental papillae at the late cap stage (15.0 dpc). *Runx3* was progressively restricted to the odontoblastic layer of tooth germ from the bell stage (17.0 dpc) to the differentiation stage, postnatal day 1 (P1) during terminal differentiation of odontoblasts (Figs.1A-D). In contrast, *Osterix* was first detected in the odontoblastic layer at 17.0 dpc, and was a more pronounced at P1 and P4 (Figs.1E-H), overlapped with *Runx3* expression. In the odontoblasts, *Bmp2* also was strongly expressed at P1 (Fig. 1O) but not *Runx2* (Fig. 1K). No positive signal was detected when using sense probe.

*Expression of Runx3 and Osterix during differentiation of the dental pulp cells into odontoblasts in vitro*

We next determined whether the mouse DPCs *in vitro* have the similar expression patterns of *Runx3 and Osterix* as those *in vivo*, RT-PCR was performed to examine gene expression of *Runx3, Osterix,* and odontoblast markers, *dentin sialophosphoprotein* (*Dspp*), *enamelysin* and *kallikrein 4* (*KLK4*) during culture (Fig. 2A). *Dspp* and *KLK4* were first detected clearly on day 21 and *enamelysin* on day 28, showing spontaneous differentiation of the DPCs into odontoblasts. *Runx3* expression was weakly detected on day 1, and increased further on day 21. *Osterix* expression was first detected on day 21 (Fig. 2A). These results correlated with *in vivo* expression during tooth development, suggesting that the DPCs might be useful for

study on the regulation of expression of *Osterix* by Runx3 at the stage before terminal differentiation of odontoblasts.

*Runx3 down-regulates Osterix expression in the mouse dental pulp cells*

To examine whether *Osterix* expression was regulated by *Runx3*, *MSCV-eGFP-Flag-Runx3* was transfected by electroporation into the mouse DPCs. Electroporation at three square-wave pulses at a frequency of 1 Hz, with a pulse length of 99 μsec and 1350 V, provided an optimal method for gene transfer *in vitro*. The cell viability was nearly 70% as determined with trypan blue, and the efficiency was nearly 35% as estimated by fluorescent microscopy. Real-time RT-PCR showed that the enhanced expression of *Runx3* mRNA, nearly 3 fold increase in the DPCs with *MSCV-eGFP-Flag-Runx3* than in control DPCs with *MSCV-eGFP* 24 hours after transfection (data not shown). Runx3 mRNA, however, were reduced to the almost same level as that of control 48 hours after transfection. On the contrary, *Osterix* expression was reduced in 25% 48 hours after transfection with *MSCV-eGFP-Flag-Runx3* compared with control transfection (Fig. 2B). These results suggest that Runx3 negatively regulates *Osx* expression in the DPCs.

*Runx3 down-regulates the Osterix promoter activity in HEK293*

A recent study has shown that *Runx2* specifically up-regulated *Osterix* promoter activity in C3H10T1/2 and ATDC5 cells, mesenchymal cell lines of bone and cartilage respectively [19]. There has been no report, however, concerning *Osterix* regulation by Runx3 so far. Runx3 shares highly conserved DNA binding domains with Runx2. Both *Runx2* and *Runx3* promoters have putative Runx binding sites that are fully conserved in sequence and location [24]. Therefore, cross-regulation between Runx2 and Runx3 might be plausible. To avoid this possible endogenous effect, HEK293 cells, in which neither *Runx2* nor *Runx3* are expressed (Fig. 3A), was used to examine transcriptional activity of Runx3.

Three putative Runx binding sites were identified on -1823 bp to -1817 bp (site 1,